

Magnetic behavior of halobis(diethyldiselenocarbamato)iron(III): Interactions, anisotropy, and three-dimensional *XY* ferromagnetism

Gary C. DeFotis and Brian K. Failon

Department of Chemistry, College of William and Mary, Williamsburg, Virginia 23185

Fred V. Wells and H. H. Wickman

Department of Chemistry, Oregon State University, Corvallis, Oregon 97331

(Received 7 November 1983)

The chloro, bromo, and iodo derivatives of the complex specified in the title have been examined by Mössbauer spectroscopy and by magnetic susceptibility and magnetization measurements. All derivatives have orbital singlet, spin quartet ground states. Mössbauer spectra are consistent with positive-*D* crystal-field parameters in each case. Cooperative transitions are observed in the chloro and bromo derivatives at 3.5 ± 0.05 and 2.7 ± 0.05 K, respectively. Below these temperatures the Mössbauer spectrum consists of a magnetic hfs component together with an unsplit quadrupole doublet whose intensity, relative to the magnetic hfs, decreases with decreasing temperature. A table of Mössbauer hyperfine parameters is presented. The principal crystal susceptibilities of the chloro and bromo derivatives have been measured over an extended temperature range, and are found to be along the [101], $(\bar{1}01)$ -normal, and [010] directions. Temperature- and field-dependent magnetization measurements along these directions are also exhibited. The anisotropy in the susceptibility and the magnetization is very large, and of *XY* character. Ferromagnetic ordering occurs at 3.463 ± 0.01 and at 2.690 ± 0.01 K in the chloro and bromo derivatives, respectively. Analysis of the susceptibility data for these two systems leads to a determination of zero-field splitting parameters, *g* values, mean exchange interactions, and anisotropy fields. An extensive table of results is displayed, and comparison is made with the corresponding series of halobis(diethyldithiocarbamato)iron(III) complexes. The temperature dependence of the reduced magnetization in the chloro and bromo derivatives, as derived from Mössbauer and magnetization measurements, is also exhibited. All the available evidence points to the conclusion that these systems are classifiable as three-dimensional *XY* ferromagnets, and that they appear to be the first known examples of this type of magnetic model system. Their *XY* character is shown to be a logical consequence of the anisotropic ground-state properties following from the observed zero-field splitting parameters. Susceptibility measurements on a powder sample of the iodo derivative reveal significant antiferromagnetic exchange interactions and permit a tentative determination of probable zero-field splitting parameters to be made. Rather curiously, this system does not order down to temperatures as low as 1.3 K. For all systems discussed here, a comparison is made between observed ordering temperatures and those predicted by available theory on the basis of measured exchange and anisotropy parameters. The relative strength of the exchange interactions in the selenocarbamato and the thiocarbamato series is also considered, as are apparent trends in the ligand dependence of the zero-field splitting parameters.

I. INTRODUCTION

The discovery of new insulating compounds whose behavior approximates that of rarely realized magnetic model systems is a major objective of modern magnetism research. Materials that exhibit strongly anisotropic magnetic properties are especially to be sought, and among these ferromagnets are particularly desirable, because relatively few are known compared to antiferromagnets. With such goals we report here an examination of the magnetic properties of important members of a new series of pentacoordinate ferric complexes, halobis(dialkyldiselenocarbamato)iron(III) (Ref. 1)—(bisdisc). A range of these complexes has been synthesized, several of which exhibit cooperative magnetic transitions.² These materials

are analogous to the corresponding series of dithiocarbamate, or bisdte complexes.^{3,4} The sulfur systems have received considerable attention owing to the orbital singlet, spin quartet ground state, 4A_2 , which is allowed by the unusual site symmetry. For several members of the series, the presence of significant intermolecular exchange interactions, in conjunction with the single-ion anisotropy, yields an interesting range of magnetic properties, with magnetic ordering in several cases and highly anisotropic behavior in certain examples of these.⁵⁻¹³ The ethyl-Cl congener, $\text{Fe}[\text{S}_2\text{CN}(\text{C}_2\text{H}_5)_2]_2\text{Cl}$, has been the most extensively studied member of the bisdte series on account of its ferromagnetism,¹⁴ extreme single-crystal anisotropy,⁹ interesting thermal^{15,9} and Mössbauer properties,^{14,16,17} and its unusual and puzzling critical behavior.^{18,19}

Nevertheless, the detailed nature of the superexchange interactions responsible for the magnetic ordering in this system remains somewhat obscure. Since the interaction is believed to operate via Fe—S···S—Fe intermolecular paths, the effects of substituting the slightly larger selenium for sulfur are worth investigating. Since low-temperature magnetic behavior often depends crucially on the detailed crystal-field anisotropy, the effects of selenium substitution in the dtc ligand of the paramagnetic Fe³⁺ ion and of halide substitution are also intriguing. Eventually, mixed-crystal studies as have already been performed on bisdtc's,^{9,10,20–22} should be worthwhile for suitable bisdsc's, and perhaps even for certain bisdsc-bisdsc combinations.

This paper describes zero-field Mössbauer and field-dependent magnetization and susceptibility measurements on the three members (Cl,Br,I) of the series halo-bis(diethyl)dsciron(III). The data are analyzed to obtain zero-field splitting parameters, *g* values, mean exchange interactions, critical temperatures, anisotropy fields, and Mössbauer hyperfine parameters. In addition, two members of the series, Fe[Se₂CN(C₂H₅)₂]₂Cl and Fe[Se₂CN(C₂H₅)₂]₂Br, appear to be examples of a heretofore unrealized class of magnetic model system, namely, three-dimensional *XY* ferromagnets (3D-*XY-F*).

II. EXPERIMENTAL

The procedures described by Cervone *et al.*¹ were employed in the synthesis of Fe[Se₂CN(C₂H₅)₂]₂Cl, hereafter Fe(dsc)₂Cl and Fe(dsc)₂Br. For Fe(dsc)₂I a method similar to that used⁴ in preparing Fe(dtc)₂I was adopted. Recrystallization from methylene chloride-toluene solutions yielded small to medium size and generally well-formed single crystals of Fe(dsc)₂Cl and Fe(dsc)₂Br. Similar recrystallizations of Fe(dsc)₂I yielded only very large grained polycrystalline material. Elemental analysis of the three materials yielded, in each case, results in excellent agreement (typically <1% relative) with expected weight percents.

Although a complete structure determination has not yet been performed on any of the bisdsc's, preliminary single-crystal diffraction data on Fe(dsc)₂Cl strongly imply that this material is isomorphous to Fe(dtc)₂Cl.²³ The molecular structure is presumably also similar, and is depicted in Fig. 1. The unit-cell parameters and probable space group of Fe(dsc)₂Cl are found to be *a*=16.81, *b*=9.61, and *c*=12.95 Å, and β=120.1°, in *P*2₁/*c* (*C*_{2h}⁵, monoclinic).²³ Those of Fe(dtc)₂Cl are known²⁴ to be *a*=16.43, *b*=9.42, and *c*=12.85 Å, and β=120.5°. The unit cell is about 5.2% larger in the dsc. Powder diffraction patterns of Fe(dsc)₂Br suggest, by comparison with the rather similar patterns of Fe(dtc)₂Br and Fe(dsc)₂Cl, that a small increase in unit-cell size also occurs between Fe(dsc)₂Cl and Fe(dsc)₂Br. It also seems likely that, as with Fe(dtc)₂Cl and Fe(dtc)₂Br,⁴ the two structures are isomorphous. The powder pattern of Fe(dsc)₂I, on the other hand, is distinctly different from any of the dtc or dsc, chloride or bromide patterns. It is also substantially different from the pattern of Fe(dtc)₂I, which is not isomorphous²⁵ to Fe(dtc)₂Cl and Fe(dtc)₂Br. Thus Fe(dsc)₂I must be assumed to crystallize in a different structure.

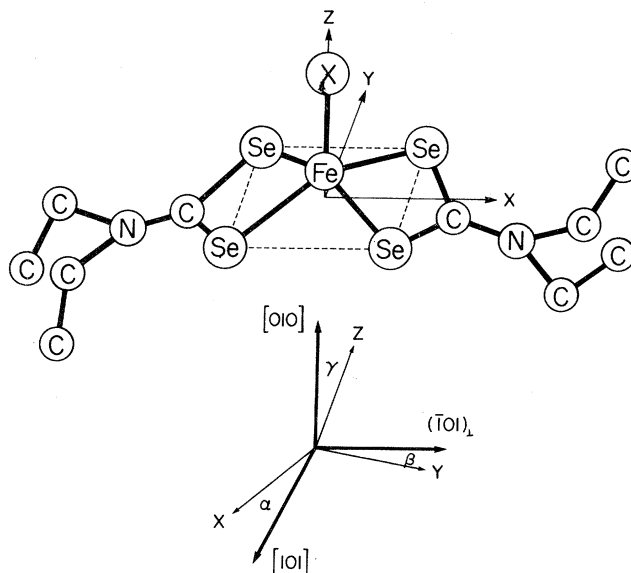


FIG. 1. Probable molecular structure, principal axes of molecular susceptibility and assumed relation to principal axes of crystal susceptibility. See text, Sec. IV.

Fe(dsc)₂Cl and Fe(dsc)₂Br crystallize from solution as prisms, elongated in the direction of the *c* axis, [001], with an unsymmetrical hexagonal cross section. The morphology is essentially identical to that of the corresponding bisdtc's. ($\bar{1}01$) is a cleavage plane. The three mutually perpendicular directions, [101], [010], and ($\bar{1}01$)-plane normal, hereafter called simply ($\bar{1}01$)_l, are easily identified and oriented. It is worth observing that unlike Fe(dtc)₂Br, which when grown from methylene chloride-toluene solution undergoes a destructive crystallographic phase transition at about 220 K, Fe(dsc)₂Br exhibits no signs of crystallographic transformation between 300 and 1.7 K.

Magnetization and susceptibility measurements were made using a Princeton Applied Research (PAR) Model 155 vibrating sample magnetometer coupled to a Janis Model 153 Superveritemp cryostat. The measuring field was provided by a 12-in.-diameter, 2-in.-gap Magnion Model 128A electromagnet and a Model HS-1365 power supply. A model FFC-4 field control unit, employing a rotating-coil gaussmeter as a probe, allowed the field to be held constant, or stepped up or down incrementally, with better than 0.01% stability over extended periods of time. Fields between 50 G and 14 kG, with homogeneity in the sample region better than 0.005%, were readily obtained. Accuracy of field settings were checked by NMR and Hall-probe measurements, and is estimated to be max(2 G, 0.1%). Temperatures were measured with a Lake Shore Cryotronics Model CGR-1-2000 carbon-glass resistance thermometer, calibrated between 1.4 and 300 K. A Lake Shore Cryotronics Model DTC-500A temperature controller permitted temperatures to be maintained constant to within 0.001–0.01 K, depending on the range. A modification of the sample holder design of PAR allowed both powder and orientation-dependent single-crystal measurements to be made.²⁶ Kel-F sample holders were employed, and data were corrected for the very small

background contributions of these and other parts of the sample rod. Single crystals were affixed to the sample holder with Apiezon grease. The magnetometer was calibrated with ferromagnetic nickel (99.999% purity) at 300 K and at 4.2 K, and with ferric ammonium sulfate between 65 and 4.2 K. Earlier measurements^{9,18} of the susceptibility and critical temperature of $\text{Fe}(\text{dsc})_2\text{Cl}$ were also checked, with agreement to within 1.5% in susceptibility and 0.003 K in T_c . It is estimated that magnetization and susceptibility data reported here are accurate to $\pm 2-3\%$, and temperatures to $\pm 0.01-0.05$ K, depending on the range.

Susceptibility measurements on $\text{Fe}(\text{dsc})_2\text{Cl}$ and $\text{Fe}(\text{dsc})_2\text{Br}$ were made in the minimum fields necessary for adequate sensitivity. Samples consisted of a collection of four of the largest well-formed single crystals available, oriented similarly and stacked parallel in mutual contact across their bc faces. The total mass was 24.25 and 8.96 mg for the chloride and bromide samples, respectively. Fields as high as 4200 G at high temperatures and as low as 100 G at low temperatures, and depending somewhat on crystal axis, were employed. In all cases, the field used at a given temperature was substantially less than a value above which departures from linearity in M vs H could be detected. Isothermal magnetization measurements, as a function of field and crystal axis, were also made on these samples. In addition, magnetization isotherms for the [101] axis were obtained using individual single crystals of $\text{Fe}(\text{dsc})_2\text{Cl}$, 2.90 mg, and $\text{Fe}(\text{dsc})_2\text{Br}$, 0.89 mg. A 43.74-mg powder sample was employed in susceptibility measurements on $\text{Fe}(\text{dsc})_2\text{I}$, with a constant measuring field of 4200 G. For this system no significant departure from linearity in M vs H could be detected at any temperature between 80 and 1.68 K in fields up to 14 kG.

Mössbauer absorbers consisted of ^{57}Fe enriched polycrystalline material mixed with boron nitride and pressed into lucite sample holders. Mössbauer spectra were recorded with a conventional, constant acceleration spectrometer. The source was ^{57}Co diffused in rhodium. All isomer shifts are referred to a natural iron foil absorber at 300 K. A Janis cryostat was used and temperatures below 4.2 K were obtained by pumping on liquid helium. Temperatures were measured by helium-vapor pressure thermometry and by a calibrated germanium resistance thermometer at the absorber, which was immersed in liquid helium.

III. MÖSSBAUER SPECTRA

At temperatures above 4 K, $\text{Fe}(\text{dsc})_2\text{Cl}$, $\text{Fe}(\text{dsc})_2\text{Br}$, and $\text{Fe}(\text{dsc})_2\text{I}$ each display simple, quadrupole doublet Mössbauer spectra with only a small temperature variation. At temperatures somewhat below 4 K, the chloro and bromo derivatives undergo cooperative magnetic transitions and develop long-range order, with $T_c = 3.5 \pm 0.05$ and 2.7 ± 0.05 K, respectively. Mössbauer spectra for these complexes are shown in Figs. 2 and 3. The iodo derivative continued to display an unsplit quadrupole doublet to the lowest temperature available (1.3 K), and is presumed therefore to undergo no magnetic ordering transition. As is typical of $S = \frac{1}{2}$ bisdsc complexes which or-

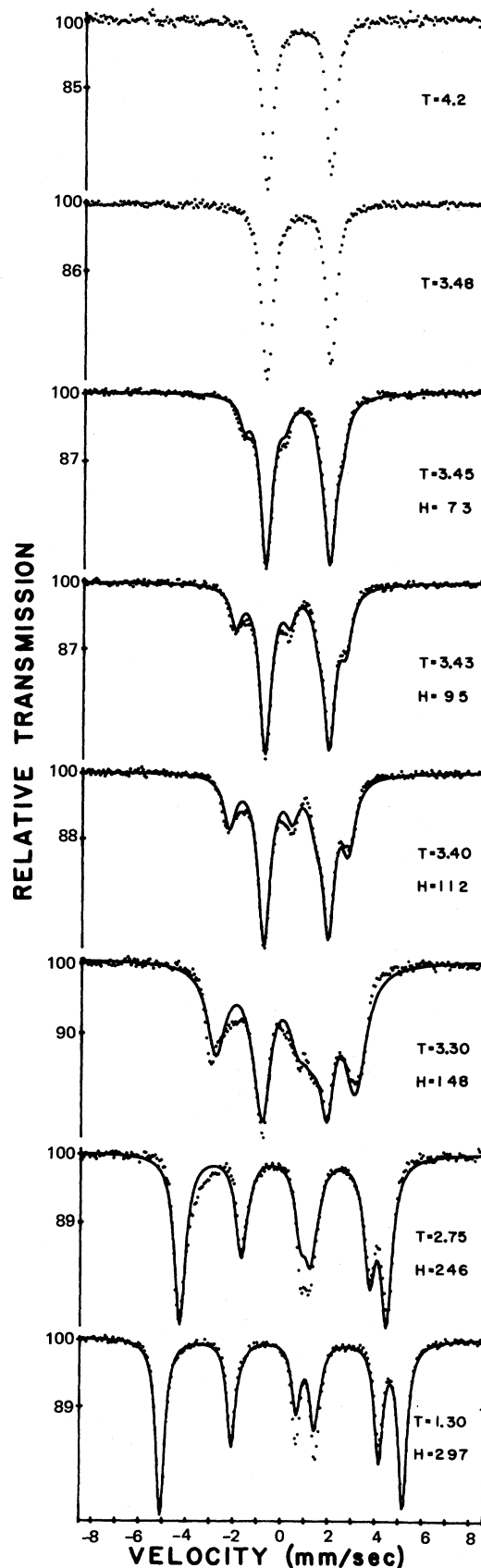


FIG. 2. Mössbauer spectra of $\text{Fe}[\text{Se}_2\text{CN}(\text{C}_2\text{H}_5)_2]_2\text{Cl}$ in zero external field. Temperatures are in K and internal fields, H , are in kG. Solid curves are computer simulations with the parameters in Table I according to the Hamiltonian Eq. (2).

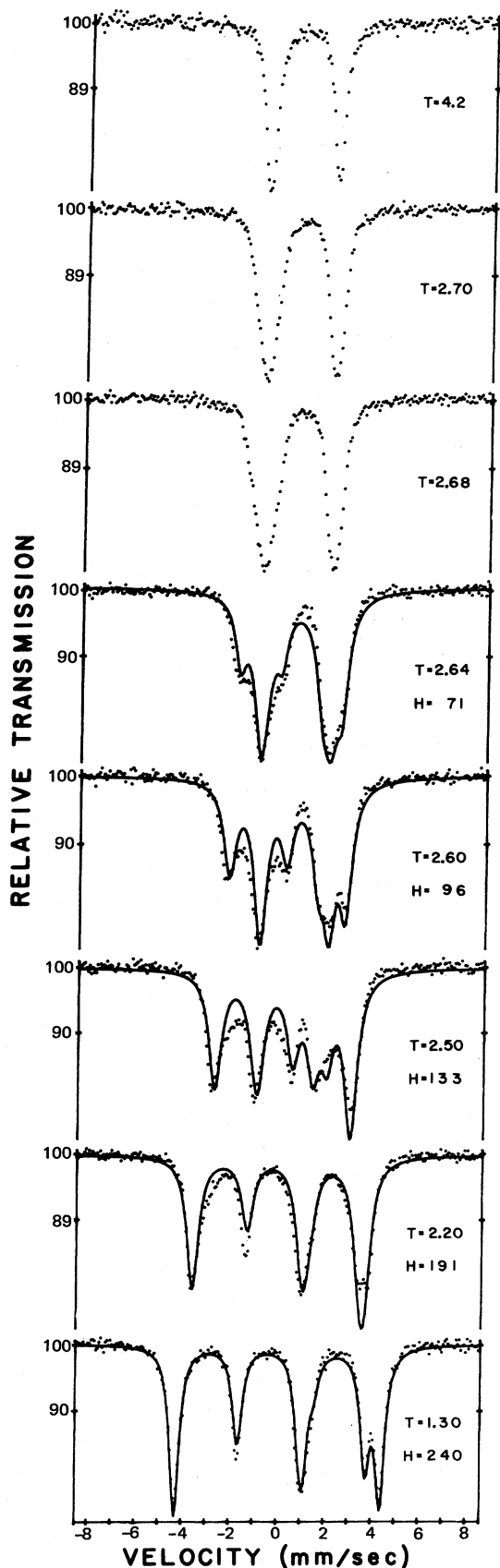


FIG. 3. Mössbauer spectra of $\text{Fe}[\text{Se}_2\text{CN}(\text{C}_2\text{H}_5)_2]_2\text{Br}$ in zero external field. Temperatures are in K and internal fields, H , are in kG. Solid curves are computer simulations with the parameters in Table I according to the Hamiltonian Eq. (2).

der magnetically, the Mössbauer spectra of $\text{Fe}(\text{dsc})_2\text{Cl}$ and $\text{Fe}(\text{dsc})_2\text{Br}$ consist of superposed quadrupole doublet and magnetic hyperfine splitting.²⁷

Electronic spectra, Mössbauer spectra, and room-temperature moments of bisdsc 's are similar to those of bisdsc 's,^{1,2} and it can be assumed that a well-isolated 4A_2 ground term occurs for the iron in the bisdsc compounds studied here. The crystal-field splittings in an $S = \frac{3}{2}$ term are described by the usual spin Hamiltonian

$$\hat{H} = D[\hat{S}_z^2 - S(S+1)/3] + E(\hat{S}_x^2 - \hat{S}_y^2). \quad (1)$$

The linewidths of the Mössbauer spectra remained sharp at all temperatures indicating fast electronic relaxation rates and a positive- D crystal-field term. Exchange interactions (discussed in detail in later sections) lead to a spin polarization that produces an effective magnetic field at the iron nucleus. The resulting Mössbauer magnetic hfs for sample temperatures of 1.30 K were fitted with an effective internal-field nuclear-spin Hamiltonian of standard form:

$$\begin{aligned} \hat{H}_{\text{hfs}} = & g_N \mu_N \vec{H}_{\text{int}}(\theta_H, \phi_H) \cdot \hat{I} + (e^2 q Q / 12) \\ & \times [3\hat{I}_z^2 - I(I+1) + \eta(\hat{I}_x^2 - \hat{I}_y^2)]. \end{aligned} \quad (2)$$

The Mössbauer hfs parameters are given in Table I. The hyperfine field H_{int} as a function of temperature also appears in Figs. 2 and 3, and in reduced form in Fig. 4. Here $M/M_0 = H_{\text{int}}(T)/H_{\text{int}}(0)$, where $H_{\text{int}}(0)$ was determined by plotting H_{int} vs T and extrapolating to $T=0$ K, yielding the estimates 306 ± 4 and 252 ± 6 kG for $\text{Fe}(\text{dsc})_2\text{Cl}$ and $\text{Fe}(\text{dsc})_2\text{Br}$, respectively.

The internal magnetic field, \vec{H}_{int} , is related to the electronic ground state of Eq. (2) by the magnetic hyperfine tensor \vec{A} . Equations (1) and (2) may be combined and written as

$$\begin{aligned} \hat{H} = & D[\hat{S}_z^2 - S(S+1)/3] + E(\hat{S}_x^2 - \hat{S}_y^2) \\ & + (e^2 q Q / 12)[3\hat{I}_z^2 - I(I+1) + \eta(\hat{I}_x^2 - \hat{I}_y^2)] \\ & + \hat{I}_x'' A_x'' \hat{S}_x'' + \hat{I}_y'' A_y'' \hat{S}_y'' + \hat{I}_z'' A_z'' \hat{S}_z''. \end{aligned} \quad (3)$$

From Eq. (3) it is clear that three coordinate systems are involved in the ground-term crystal-field and hyperfine interactions. The electric-field-gradient system (x', y', z') is correlated with molecular structure; V_{zz} is parallel to the iron-halide direction.^{28,29} It is likely, but not *a priori* certain, that the \vec{A} tensor will also correlate with molecular geometry.²⁸ Further, the \vec{A} tensor is not isotropic in $\text{Fe}(\text{dsc})_2\text{X}$ and $\text{Fe}(\text{dsc})_2\text{X}$ complexes.³⁰ The orientation of the crystal-field tensor (x, y, z) is not deducible from polycrystalline Mössbauer spectra, nor can it be reliably correlated with molecular geometry on theoretical grounds. Therefore, in so far as zero-field powder Mössbauer spectra are concerned, the parameters in Eq. (3) are highly undetermined.

More information can be obtained from magnetically perturbed Mössbauer spectra, which will be reported and analyzed separately.³⁰ The result of most relevance to this work is that the exchange field in $\text{Fe}(\text{dsc})_2\text{Cl}$, which can be induced above T_c by an applied field, attains a max-

TABLE I. Mössbauer hyperfine parameters for bis(diethylselenocarbomato)iron(III) halides. Values in parentheses are estimated uncertainties in the last significant digit(s).

System	T (K)	δE (mm/sec)	ΔE_Q (mm/sec)	η	T_c (K)	H_{int} (kG)	θ_H (deg)	ϕ_H (deg)
Fe(dsc) ₂ Cl	1.3	0.565(3)	2.71(3)	0.13	3.50(5)	297(3)	90(10)	0(10)
	77	0.550(3)	2.70(3)					
Fe(dsc) ₂ Br	1.3	0.544(3)	2.89(3)	0.05	2.70(5)	240(3)	90(10)	0(10)
	77	0.546(3)	2.91(3)					
Fe(dsc) ₂ I	1.3	0.530(3)	3.01(3)					
	77	0.528(3)	3.03(3)					

imum value of 31.5 ± 1.5 kG for $H_{\text{app}} \geq 10$ kG. Moreover, it appears to be directed nearly along the x axis of Fig. 1, and somewhat out of the x - y plane. A similarly directed exchange field, of magnitude 15 ± 1 kG, appears to yield a good fit to magnetically perturbed Mössbauer spectra of Fe(dtc)₂Cl. Additional quantitative information concerning crystal-field splittings (D, E) are most directly obtained from single-crystal magnetization data which are now discussed.

IV. MAGNETIC SUSCEPTIBILITY

Magnetic susceptibilities measured along three orthogonal crystal directions, $[101]$, $(\bar{1}01)_1$, and $[010]$, are shown in Figs. 5 and 6, for Fe(dsc)₂Cl and Fe(dsc)₂Br, respectively. The data are uncorrected for demagnetization. The very large susceptibility observed along $[101]$, and the smaller but still large susceptibility along $(\bar{1}01)_1$, are clearly indicative of very substantial ferromagnetic interactions, and of eventual ferromagnetic ordering. Noteworthy is the pronounced anisotropy. Near and just above the ordering temperatures (to be discussed) the ratio $\chi_{[101]}:\chi_{(\bar{1}01)_1}:\chi_{[010]}$ is 150:25:1 and 100:33:1 for the chloride and bromide, respectively. The degree of anisotropy is reminiscent of that in Fe(dtc)₂Cl.⁹ However, in that case the susceptibility attained a very large value *only* along $[101]$, remaining much smaller along $(\bar{1}01)_1$ and $[010]$ with magnitude comparable to those observed along $[010]$ here. But just as for Fe(dtc)₂Cl, the principal axes

of the crystal susceptibility tensors of Fe(dsc)₂Cl and Fe(dsc)₂Br are found to be $[010]$, $[101]$, and $(\bar{1}01)_1$. The twofold b axis, $[010]$, must be one of the principal axes, and this is confirmed experimentally. By rotating the driver head of the magnetometer, with the samples mounted so that $[010]$ is parallel to the axis of rotation, the principal axis directions $[101]$ and $(\bar{1}01)_1$ were easily determined to within an experimental uncertainty of about 3° .

The large size and leveling behavior of $\chi_{[101]}$ below T_c suggests that $[101]$ is the easy axis of ferromagnetic ordering. The somewhat gradual approach to a value independent of temperature is due to two factors. First, the crystals employed in the measurements are platelike in shape (the materials are not readily worked into ellipsoids of revolution) so that a unique demagnetization factor does not exist. Second, each of the samples consisted of four not quite identically shaped crystals, so that there is a range of effective demagnetization factors in each case. Nevertheless, the apparent demagnetization factor along $[101]$, taken to be equal to the reciprocal of the estimated volume susceptibility when leveled below T_c , is a quite reasonable $N_{[101]} = 3.56$ and 3.36 for Fe(dsc)₂Cl and Fe(dsc)₂Br, respectively. In obtaining the value of N for the bromide, the density was calculated assuming that the unit-cell size is 1.029 times that of Fe(dsc)₂Cl, which is the relation between Fe(dtc)₂Cl and Fe(dtc)₂Br. From the relative dimensions of the average crystal of each sample along $[101]$, $[010]$, and $(\bar{1}01)_1$, and assuming that $N_{[101]} + N_{(\bar{1}01)_1} + N_{[010]} = 4\pi$, the demagnetization factors

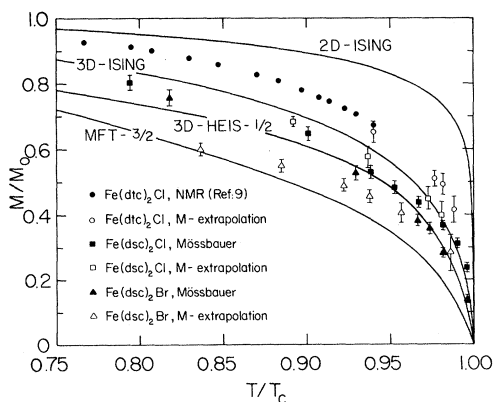


FIG. 4. Reduced magnetization vs reduced temperature for Fe[Se₂CN(C₂H₅)₂]₂Cl, Fe[Se₂CN(C₂H₅)₂]₂Br, and Fe[S₂CN(C₂H₅)₂]₂Cl, obtained by various methods. Solid curves are predictions according to simple theoretical models.

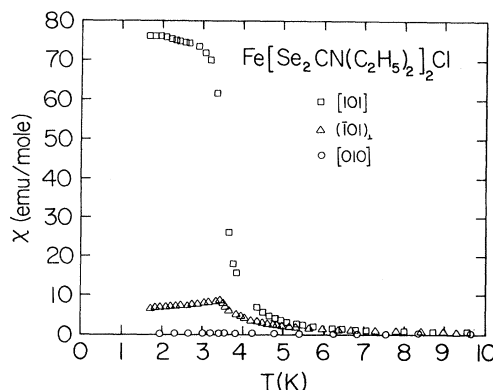


FIG. 5. Principal crystal susceptibilities of Fe[Se₂CN(C₂H₅)₂]₂Cl, before correction for demagnetization.

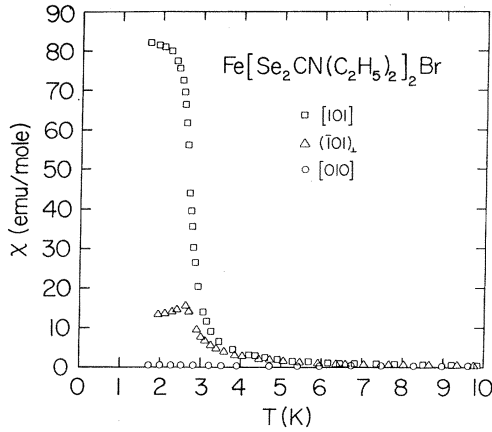


FIG. 6. Principal crystal susceptibilities of $\text{Fe}[\text{Se}_2\text{CN}(\text{C}_2\text{H}_5)_2]_2\text{Br}$, before correction for demagnetization.

$N_{[010]}=4.0, 6.2$ and $N_{(\bar{1}01)_\perp}=5.0, 3.0$ for $\text{Fe}(\text{dsc})_2\text{Cl}$ and $\text{Fe}(\text{dsc})_2\text{Br}$, respectively, were estimated. Corrected molar susceptibilities, Figs. 7 and 8, to be used in subsequent analysis are obtained from the usual expression,⁹

$$\chi_M = \chi_{M,\text{unc}} / [1 - N(\rho/M')\chi_{M,\text{unc}}],$$

where unc is uncorrected, and where N is the appropriate demagnetization factor, ρ is the density, and M' is the molecular weight. It should be emphasized that even fairly substantial potential errors in the demagnetization factors will have an almost negligible effect on later results.

An estimate of the value of T_c can be obtained from the data of Fig. 7 by noting that peaks in each of $\chi_{[010]}$ and $\chi_{(\bar{1}01)_\perp}$ occur at 3.42 ± 0.01 K for $\text{Fe}(\text{dsc})_2\text{Cl}$. For $\text{Fe}(\text{dsc})_2\text{Br}$ a peak appears only in $\chi_{(\bar{1}01)_\perp}$, at 2.62 ± 0.01 K. In earlier work on $\text{Fe}(\text{dsc})_2\text{Cl}$,⁹ peaks in $\chi_{[010]}$ and $\chi_{(\bar{1}01)_\perp}$ were observed at 2.50 ± 0.01 and 2.46 ± 0.01 K, respectively, near but somewhat above the critical temperature, 2.45_7 K, determined from a fit¹⁸ to $\chi_{[101]}$ data according to the asymptotic power-law form, $\chi_0 = \Gamma[(T - T_c)/T_c]^{-\gamma}$. The rms applied field was a rather small

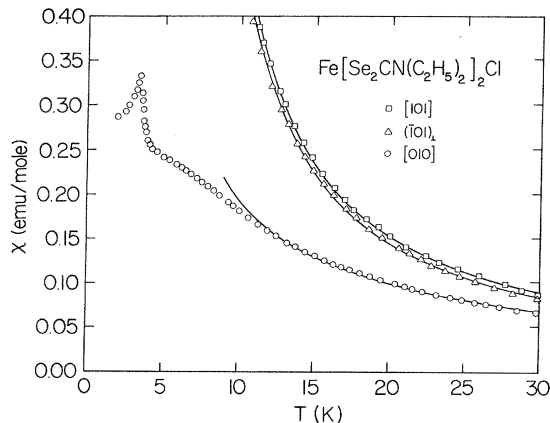


FIG. 7. Principal crystal susceptibilities of $\text{Fe}[\text{Se}_2\text{CN}(\text{C}_2\text{H}_5)_2]_2\text{Cl}$, after correction for demagnetization. Solid curves are the best fit to the data with the parameters appearing in Table II.

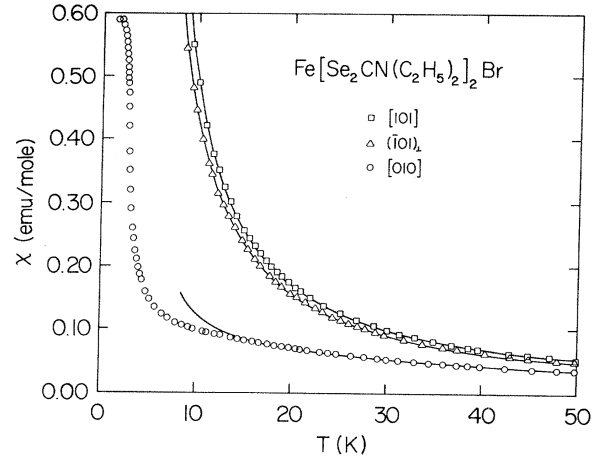


FIG. 8. Principal crystal susceptibilities of $\text{Fe}[\text{Se}_2\text{CN}(\text{C}_2\text{H}_5)_2]_2\text{Br}$, after correction for demagnetization. Solid curves are the best fit to the data with the parameters appearing in Table II.

12 G in these earlier measurements. Here the applied field is somewhat greater. Results to be discussed in Sec. V show that a small field of 100 to 300 G depresses the ordering temperature by several 0.01 K. The true values of T_c appear to be 3.463 ± 0.003 and 2.690 ± 0.005 K for $\text{Fe}(\text{dsc})_2\text{Cl}$ and $\text{Fe}(\text{dsc})_2\text{Br}$, respectively, in agreement with the zero-field Mössbauer data. The absence of a peak in $\chi_{[010]}$ for $\text{Fe}(\text{dsc})_2\text{Br}$, leveling behavior being observed instead (Fig. 8), is also noticeable. Magnetization data in Sec. V suggest that a small ferromagnetic (F) component of moment develops along [010] in the bromide. It is uncertain whether this is intrinsic or related to slight misorientations or crystal imperfections.

As noted above, the effects of axial and rhombic crystal-field distortions and an applied field on the ground term are described by the Hamiltonian

$$\hat{H} = D[\hat{S}_z^2 - S(S+1)/3] + E[\hat{S}_x^2 - \hat{S}_y^2] + \mu_B(g_x H_x \hat{S}_x + g_y H_y \hat{S}_y + g_z H_z \hat{S}_z). \quad (4)$$

In zero field the eigenvalues³¹ consists of a pair of Kramers doublets separated by an energy difference $\delta = 2(D^2 + 3E^2)^{1/2}$. If $D > 0$ and $|E/D|$ is small, the ground doublet is essentially $|\pm \frac{1}{2}\rangle$, with the upper doublet $|\pm \frac{3}{2}\rangle$. For $D < 0$ the situation is reversed. The observed susceptibilities above the ordering temperatures will be accounted for in terms of single-ion contributions to a total crystal susceptibility, enhanced by exchange interaction in a mean-field approximation. The partition function

$$Z = \sum_{j=1}^4 \exp(-E_j/kT) \quad (5)$$

may be evaluated, and since

$$\chi_i = (kT/H)[\partial \ln Z_i / \partial H], \quad (6)$$

where $i = x, y, \text{ or } z$ for the cases $H \parallel x, H \parallel y, \text{ or } H \parallel z$, respectively, one finds after some algebra⁶

$$\chi_i = \left[\frac{N_0 g_i^2 \mu_B^2}{kT} \right] \left[\left[\frac{4A_i^2}{\delta^2} + \frac{1}{4} \right] + \left[\frac{24B_i^2}{r\delta^2} - \frac{2A_i}{\delta} \right] \left[\frac{1-e^{-r}}{1+e^{-r}} \right] \right], \quad (7)$$

where $r = \delta/kT$ and where $A_x = (3E - D)/2$, $A_y = -(3E + D)/2$, $A_z = D$, and $B_x = (D + E)/2$, $B_y = (D - E)/2$, $B_z = E$.

In order to relate the measured susceptibilities along [010], [101], and $(\bar{1}01)_\perp$ to the single-ion susceptibilities χ_x , χ_y , and χ_z , the relative orientation of the two sets of principal axes is needed. Based on the chemical and structural similarities of $\text{Fe}(\text{dsc})_2\text{Cl}$ and $\text{Fe}(\text{dte})_2\text{Cl}$ noted in Sec. II, it will be assumed that the same relationships occur for $\text{Fe}(\text{dsc})_2\text{Cl}$ and for $\text{Fe}(\text{dsc})_2\text{Br}$ as for their bisdte analogs. This means taking $\alpha = 20.7^\circ$, $\beta = 4.0^\circ$, and $\gamma = 21.1^\circ$, each $\pm 0.1^\circ$, in the lower part of Fig. 1, valid for one of the four molecules in the unit cell (with relations for the other three molecules determined by symmetry). The choice of x , y , and z molecular principal axes in Fig. 1 is that which leads to the most self-consistent set of parameters in the fit to both susceptibility and Mössbauer data, to be explained. It is possible that full structure determinations might reveal variations in the assumed angles of as much as a few degrees. Deviations of this magnitude will have only a slight influence of the parameter values obtained in the following. A crystal susceptibility χ_k is related to single-ion principal susceptibilities $\chi_{i,m}$ by

$$\chi_k = \sum_{i,m} \chi_{i,m} C_{ik,m}^2 \{ i = x, y, z; k = [010], [101], (\bar{1}01)_\perp \}, \quad (8)$$

where $C_{ik,m}$ is the direction cosine between axes i and k for molecule m , and where m runs from 1 to 4. This relation assumes that the susceptibility is a second-rank tensor, and is valid provided that the measuring field (Sec. II) is sufficiently small so that the magnetization is proportional to the susceptibility.

If one attempts to account for the observed susceptibilities in terms of single-ion contributions alone, Eqs. (7) and (8), calculated values are substantially below observed values for any reasonable choice of parameters and the fit is poor even at high temperatures. A ferromagnetic exchange enhancement of the susceptibility is obviously occurring. In sufficiently low fields, where the field-induced polarization is not large, this enhancement can be introduced via a molecular-field approximation, in which the interaction of ion i with its z neighbor ions j is taken to be $\hat{H}_{\text{ex}} = -2zJ\hat{S}_i \cdot \langle \hat{S}_j \rangle$. J is positive for ferromagnetic exchange and negative for antiferromagnetic. The calculated susceptibility with exchange effects included, χ_i^{ex} , is related to that obtained neglecting exchange, χ_i , by³²

$$\chi_i^{\text{ex}} = \chi_i [1 - (2zJ/N_0 g_i^2 \mu_B^2) \chi_i]^{-1}. \quad (9)$$

Without a detailed picture of the different exchange interactions that occur between specific numbers of near

and next-nearest neighbors, it is of course only an effective interaction over z neighbors, zJ , that will be obtained.

Equations (7)–(9) contain six independent parameters, D , E , g_x , g_y , g_z , and zJ . Three independent principal crystalline susceptibilities and their detailed temperature dependences are available. Previous experience with $\text{Fe}(\text{dte})_2\text{Cl}$ and other systems shows that a unique determination of optimal values for these parameters is possible. A nonlinear least-squares fitting program was employed to search parameter space for the best values, with all available data being fit simultaneously. Excellent fits to the data in the ranges 30–11 K for $\text{Fe}(\text{dsc})_2\text{Cl}$, Fig. 7, and 50–13 K for $\text{Fe}(\text{dsc})_2\text{Br}$, Fig. 8, were obtained, with rms deviations in χ of 1.2% and 1.3%, respectively. The fitted parameters are shown in Table II, along with values determined earlier for corresponding bisdte's. The indicated uncertainties are conservative estimates that take account of potential systematic errors in T , χ , demagnetization, and molecular orientation. The lowest-temperature data included in the fitting were those for which the quality of fit remained similar to what it was when this minimum temperature was 1–2 K higher. Attempting to fit still lower-temperature data led to a more significant deterioration in the quality of fit. This was also the procedure employed earlier for $\text{Fe}(\text{dte})_2\text{Cl}$.⁹ In each of these three cases it is found that the fitting cannot be satisfactorily continued below a temperature about six times larger than zJ/k , and smaller than the zero-field splitting δ/k . At lower temperatures the calculated susceptibility increases too rapidly, especially along [010]. We believe that this behavior is due primarily to the increasingly unsatisfactory nature of the mean-field approximation in the form employed as the upper Kramers doublet is depopulated, and as the effective exchange anisotropy arising from the anisotropic character of the lower doublet becomes more pronounced.

In arriving at the parameter values shown in Table II, many different combinations of initial values were employed. These included values well away from, and either smaller or greater than, those finally obtained. Thus it is believed that a true minimum in parameter space has been located in the reported fits, and this is to some extent confirmed by the physically reasonable values obtained. Note that $|E|$ is quite small compared to $|D|$, indicating that departures from axial symmetry are not large, and substantially less than in $\text{Fe}(\text{dte})_2\text{Cl}$. It can be shown³³ that with a correct choice of principal axes, $|E/D| \leq \frac{1}{3}$ is always satisfied. Two other natural choices of molecular principal axes correspond to the cyclic permutations $xyz \rightarrow yzx$ or zyx [as in $\text{Fe}(\text{dte})_2\text{Cl}$] in the upper part of Fig. 1. With either of these alternative assignments of quantization axes equally good fits can be obtained. The g values are very similar, though permuted, and zJ is the same. However, D and E assume very different values, and though they yield the same value of δ , the $|E/D| \leq \frac{1}{3}$ criterion is violated. It is also confirmed that permutations of the principal axes of the zero-field splitting tensor, with elements $\delta_{xx} = E - D/3$, $\delta_{yy} = -(E + D/3)$, and $\delta_{zz} = 2D/3$,³³ yield the same pairs of D and E values obtained in the fitting attempts with yzx or zyx assignments. As an additional check, the only

TABLE II. Magnetic parameters characterizing some iron(III)-halide bisdsc and bisdtd systems. Values in parentheses are estimated uncertainties in the last significant digit(s). Values in brackets are considered to be of inherently greater uncertainty due to the method of their determination.

System	D/k (K)	E/k (K)	δ/k (K)	g_x	g_y	g_z	$\beta J/k$ (K)	H_E (G)	H_A (G)	H'_A (G)	α	α'	T_c (K)
Fe(dsc) ₂ Cl	6.95(10)	-0.14(5)	13.91(20)	2.14(3)	2.05(3)	2.09(3)	1.85(5)	38 600(1200)	62 600(3000)	2500(150)	1.6(1)	0.065(5)	3.463(3)
Fe(dsc) ₂ Br	15.74(20)	-0.29(5)	31.50(40)	2.20(3)	2.07(3)	2.07(3)	1.85(5)	37 600(1200)	29 600(1400)	1600(100)	0.79(5)	0.043(3)	2.690(5)
Fe(dsc) ₂ I	[11.5(1.0)]	[-0.45(20)]	[23.05(2.0)]	[2.20(5)]	[2.10(5)]	[2.03(5)]	[-1.55(5)]						
Fe(dtc) ₂ Cl ^a	-3.32(5)	-0.65(5)	7.01(15)	2.09(3)	2.10(3)	2.12(3)	0.81(5)	17 100(1100)	65 900(3000)	26 600(1300)	3.9(3)	1.6(1)	2.460(7)
Fe(dtc) ₂ Br ^b	10.78(30)	-0.72(15)	21.71(60)	2.07(5)	2.04(5)	[2.00]	[0.8(3)] ^c	[17 000(6000)]					1.347(9) ^d
Fe(dtc) ₂ I ^b	13.46(5)	-2.55(20)	28.33(30)	2.08(5)	2.05(5)	[2.00]	[-0.8(3)] ^e	[17 000(6000)]					1.52(2) ^f

^aReference 9.

^bReference 6.

^cEstimated from observed Weiss Θ using Eq. (21).

^dReference 13.

^eReference 11.

^fReference 12.

off-diagonal element of the crystal susceptibility tensor which is not equal to zero by symmetry, $\chi_{[101],(\bar{1}01)}$ was calculated and found to be less than 1% of the diagonal elements. Possible misorientation of the assumed molecular principal axes, due to departures of molecular orientations from those assumed, probably does not exceed 5°.

Powder susceptibility data for Fe(dsc)₂I appear in Fig. 9. It is evident that χ_M^{-1} is linear in T over a considerable range of temperature. Data between 30 and 80 K conform well to a Curie-Weiss expression,

$$\chi_M = C/(T - \Theta), \quad (10)$$

with $C=2.077$ emu K mole⁻¹ and $\Theta=-3.52$ K. Since $C=N_0g^2\mu_B^2S(S+1)/3k$ and $S=\frac{3}{2}$, one calculates $g_{av}=2.105$. The negative Θ value indicates that the iodide, in contrast to the chloride and bromide, is characterized by predominantly antiferromagnetic interactions. However, there is no indication of (antiferromagnetic) ordering as low as 1.7 K, or even 1.3 K (Mössbauer). Fe(dtc)₂I, on the other hand, is known to order antiferromagnetically at 1.94 K,^{5,12} and its Weiss Θ is about -2 K.⁵ This comparison provides an additional indication that the structures of the iodide systems are not the same.

Below 30 K significant departures from the Curie-Weiss dependence are observed. An attempt has been made to account for these data by applying the theoretical formalism used for Fe(dsc)₂Cl and Fe(dsc)₂Br. Since only powder data are available, the calculated susceptibilities must be averaged and the absence of knowledge regarding the crystal structure and molecular orientations is not a handicap. If it is assumed that g is isotropic, then a comparatively simple expression for

$$\chi_{av} = (\chi_x + \chi_y + \chi_z)/3 \quad (11)$$

can be obtained from the general results, Eq. (7); it takes the form

$$\chi_{av} = (N_0g_{av}^2\mu_B^2/kT) \left[\frac{3}{4} + r^{-1}(1 - e^{-r})/(1 + e^{-r}) \right]. \quad (12)$$

Thus one might expect to be able to deduce a mean g value and the zero-field splitting from powder data over a sufficiently extended temperature range. Because the interactions in the present case are rather substantial, it is also necessary to include a mean-field correction for exchange, Eq. (9), in order to fit the observed susceptibilities. It is found that with $g_{av}=2.11$, $\delta/k=23$ K, and $\beta J/k=-1.5$ K, the data can be nicely accounted for (rms deviation of 1.0%) between 80 and 15 K. At lower temperatures the calculated values are as much as 10% too high. An attempt was therefore made to allow for g anisotropy and to fit all six parameters of Eqs. (7) and (9). An excellent fit to all data between 1.7 and 80 K was obtained (rms deviation of 1.0% overall, 1.5% below 15 K) with the parameters listed in Table II. The fit is reproduced in Fig. 9. Despite the apparent success, we are reluctant to claim the same degree of reliability for parameters deduced from powder data, and therefore the values are given in brackets in the table.

The anisotropy in the susceptibilities of Fe(dsc)₂Cl and

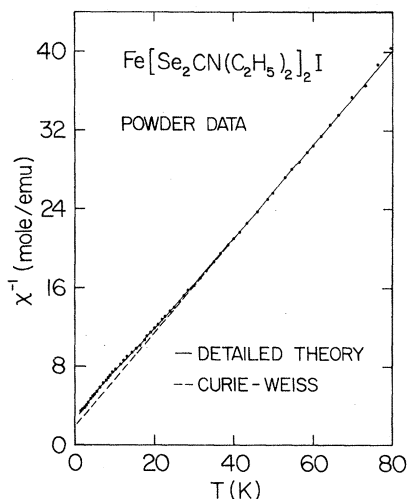


FIG. 9. Inverse magnetic susceptibility of polycrystalline $\text{Fe}[\text{Se}_2\text{CN}(\text{C}_2\text{H}_5)_2]_2\text{I}$ corrected for demagnetization and diamagnetism. Curie-Weiss fit and detailed theory fit are described in text, with parameters in Table II.

$\text{Fe}(\text{dsc})_2\text{Br}$ below T_c can be used to estimate effective anisotropy fields which characterize these materials. Molecular-field theory yields an expression for the susceptibility of a ferromagnet at 0 K along a hard or next preferred axis i ,³⁴

$$\chi_i(0) = (N_i + H_A^i / N_0 g_i \mu_B S)^{-1}, \quad (13)$$

where N_i is the demagnetization factor along axis i and H_A^i is the anisotropy field associated with this axis. The (uncorrected) susceptibilities along $(\bar{1}01)_1$ and $[010]$ can be extrapolated to 0 K to estimate $\chi_{(\bar{1}01)_1}(0) = 6.1, 9.8$ emu mole⁻¹ and $\chi_{[010]}(0) = 0.279, 0.579$ emu mole⁻¹ for the chloride and bromide, respectively, in each case with an uncertainty of about 4%. Converting these values to per unit volume dimensions and using the demagnetization factors estimated earlier, one obtains the anisotropy fields given in Table II. Here H_A and H'_A are associated with the hard axis and with the next preferred axis, respectively, and are sometimes referred to as out-of-plane and in-plane anisotropy fields.³⁵ Molecular-field theory also yields for the exchange field

$$H_E = 2z |J| S / g \mu_B, \quad (14)$$

where g is along the easy axis.³⁵ H_E appears in Table II, as do the useful measures of relative anisotropy, $\alpha = H_A / H_E$ and $\alpha' = H'_A / H_E$. Further discussion of these results will be given in Sec. VI.

V. MAGNETIZATION

Magnetization as a function of applied field, temperature, and crystal axis is shown in Figs. 10 and 11 for $\text{Fe}(\text{dsc})_2\text{Cl}$ and $\text{Fe}(\text{dsc})_2\text{Br}$, respectively. It is apparent from these data that both systems are ferromagnetic, that $[010]$ is a hard axis, and that the (010) plane is an easy plane, with $[101]$ the preferred axis in this plane. Near saturation along $[101]$ and $(\bar{1}01)_1$ in $\text{Fe}(\text{dsc})_2\text{Cl}$ appears to be achieved at 14 kG and 1.7–1.8 K ($T/T_c = 0.5_0$).

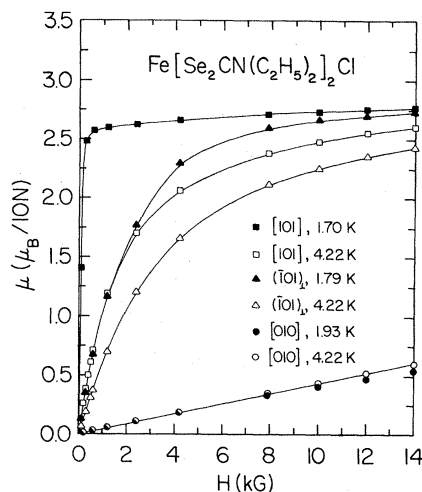


FIG. 10. Observed magnetization above and below $T_c = 3.46$ K along the principal axes of $\text{Fe}[\text{Se}_2\text{CN}(\text{C}_2\text{H}_5)_2]_2\text{Cl}$. Solid curves are guides to the eye.

This is somewhat less apparent for $\text{Fe}(\text{dsc})_2\text{Br}$, due presumably to the larger reduced temperature of about 0.7₃. It is estimated that $\mu_{\text{sat}} = (2.85 \pm 0.05) \mu_B/\text{ion}$ and $(2.75 \pm 0.05) \mu_B/\text{ion}$ for the chloride and bromide, respectively.

In $\text{Fe}(\text{dsc})_2\text{Cl}$, the magnetization, $M_{[010]}$, is almost linear in H , to 14 kG, even below T_c . In $\text{Fe}(\text{dsc})_2\text{Br}$ some curvature in $M_{[010]}$ at relatively low field is evident for $T < T_c$, but above 3 kG the magnetization is linear in H . Small misalignments due to crystal imperfections may be responsible for the low-field curvature. From the intersection of the linear portions (at low field and at high field) of the magnetization isotherms along $[101]$ and $(\bar{1}01)_1$, it is possible to estimate the demagnetizing and anisotropy fields.³⁶ The intersections are at 205 and 170 G along $[101]$, and at 2260 and 1010 G along $(\bar{1}01)_1$, for $\text{Fe}(\text{dsc})_2\text{Cl}$ and $\text{Fe}(\text{dsc})_2\text{Br}$, respectively, with at least 5% uncertainties. The $[101]$ values are in excellent agreement

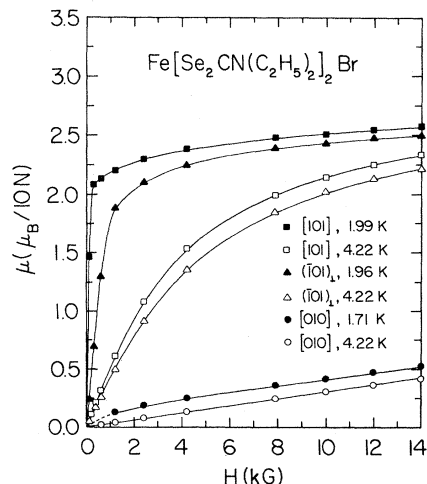


FIG. 11. Observed magnetization above and below $T_c = 2.69$ K along the principal axes of $\text{Fe}[\text{Se}_2\text{CN}(\text{C}_2\text{H}_5)_2]_2\text{Br}$. Solid curves are guides to the eye.

with the demagnetizing fields calculated ($H_d = NM$) from the observed magnetizations and the values of $N_{[101]}$ estimated earlier, 194 and 161 G for the chloride and bromide, respectively. Subtracting the similar demagnetizing fields along $(\bar{1}01)_\perp$ from the observed intersections for this axis yields $H'_d = 2000$ and 870 G, each $\pm 5\%$, for $\text{Fe}(\text{dsc})_2\text{Cl}$ and $\text{Fe}(\text{dsc})_2\text{Br}$, respectively. These values are somewhat smaller than the 0 K values estimated from susceptibility data listed in Table II. This is not unreasonable, however, since it is known that anisotropy constants can vary strongly with temperature.³⁷ The essential linearity of the [010] data suggests that the anisotropy fields H_A for $\text{Fe}(\text{dsc})_2\text{Cl}$ and $\text{Fe}(\text{dsc})_2\text{Br}$, associated with the [010] axis, are each in excess of 12–14 kG, consistent with the susceptibility-derived values in Table II.

In order to obtain reliable estimates of the transition temperatures for $\text{Fe}(\text{dsc})_2\text{Cl}$ and $\text{Fe}(\text{dsc})_2\text{Br}$, and information on the spontaneous magnetization as a function of temperature, the magnetization along [101] in small single-crystal samples was measured as a function of field and temperature above and below T_c . The results are shown in Figs. 12 and 13, as isotherms of M^2 vs H/M , where H is the internal field, $H_{\text{app}} - NM$. The rationale of such Kouvel-Arrott plots is well known.³⁸ The intersection of a $T > T_c$ isotherm with the H/M axis, $(H/M)_0$, is the inverse initial (zero-field) susceptibility; for $T = T_c$ the expected value is $(H/M)_0 = 0$. The extrapolation of a $T < T_c$ isotherm to $H/M = 0$ (employing data taken at low fields in excess of the demagnetizing field) yields a value for the square of the spontaneous magnetization. In Fig. 14 are shown the values of $(H/M)_0$ as a function of temperature for $\text{Fe}(\text{dsc})_2\text{Cl}$ and $\text{Fe}(\text{dsc})_2\text{Br}$, and also for $\text{Fe}(\text{dsc})_2\text{Cl}$ for purposes of comparison. Fairly reliable extrapolations to $(H/M)_0 = 0$ are possible, and yield the critical temperatures shown in the figure and in Table II. The result for $\text{Fe}(\text{dsc})_2\text{Cl}$ is in excellent agreement with that obtained previously^{18,19} from the critical behavior of the near-zero-field susceptibility, $T_c = 2.457 \pm 0.005$ K.

The spontaneous magnetization as a function of temperature for $\text{Fe}(\text{dsc})_2\text{Cl}$ and $\text{Fe}(\text{dsc})_2\text{Br}$, deduced from the data in Figs. 12 and 13, appears in Fig. 4. Also shown are results for $\text{Fe}(\text{dsc})_2\text{Cl}$ obtained by the same method. In

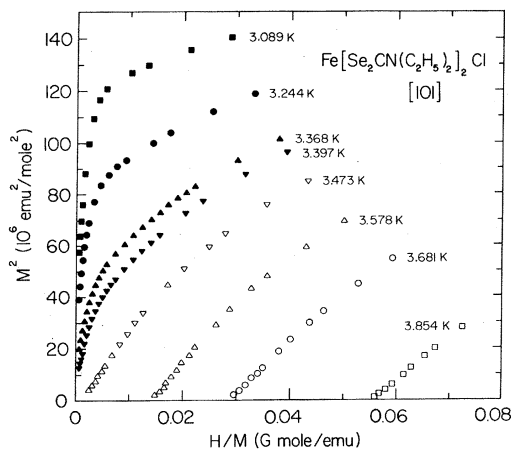


FIG. 12. Kouvel-Arrott plot for $\text{Fe}[\text{Se}_2\text{CN}(\text{C}_2\text{H}_5)_2]_2\text{Cl}$ single-crystal data along [101]. H is the internal field.

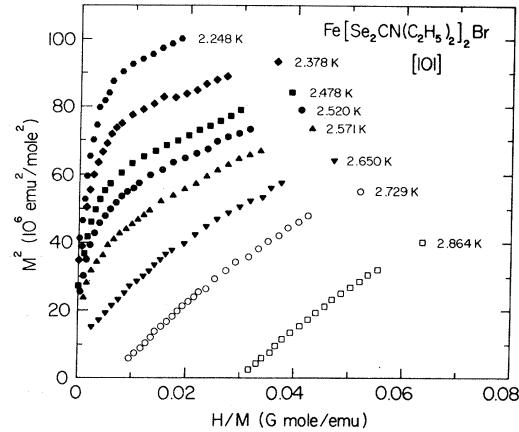


FIG. 13. Kouvel-Arrott plot for $\text{Fe}[\text{Se}_2\text{CN}(\text{C}_2\text{H}_5)_2]_2\text{Br}$ single-crystal data along [101]. H is the internal field.

each case the reduced magnetization M/M_0 is obtained by dividing the extrapolated value of $(M^2)^{1/2}$ at $H/M = 0$ by the estimated saturation magnetization from high-field measurements: $\mu_{\text{sat}} = 2.85\mu_B/\text{ion}$, $2.75\mu_B/\text{ion}$, and $3.12\mu_B/\text{ion}$ for $\text{Fe}(\text{dsc})_2\text{Cl}$, $\text{Fe}(\text{dsc})_2\text{Br}$, and $\text{Fe}(\text{dsc})_2\text{Cl}$, respectively. The value of μ_{sat} for $\text{Fe}(\text{dsc})_2\text{Cl}$ is about 5% lower than a result obtained previously employing a different apparatus,¹⁰ and is believed to be more accurate.

VI. DISCUSSION

For both $\text{Fe}(\text{dsc})_2\text{Cl}$ and $\text{Fe}(\text{dsc})_2\text{Br}$ the anisotropy in the principal crystal susceptibilities as a function of temperature, and in the magnetization along three orthogonal crystal directions as a function of field, are suggestive of XY model behavior. None of the data display features typical of two-dimensional (2D) lattice systems, nor does the crystal structure [presumably isomorphous to that of $\text{Fe}(\text{dsc})_2\text{Cl}$] exhibit any obvious lattice anisotropy. Therefore, it is likely that each of these systems belongs to the universality class of three-dimensional XY ferromagnets (3D- XY -F). Indeed, they appear to be the first such examples, previously examined XY -F systems having been either 2D,^{39–42,36} or 1D,^{43,44} and previously examined 3D-

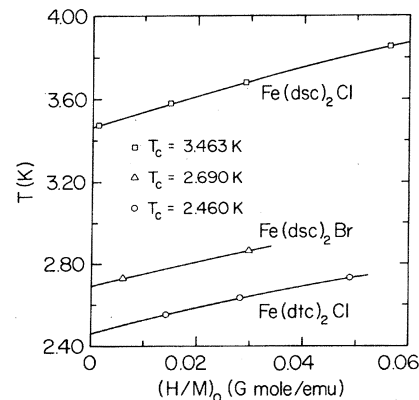


FIG. 14. Inverse initial susceptibility, $(H/M)_0$, as a function of temperature for $\text{Fe}[\text{Se}_2\text{CN}(\text{C}_2\text{H}_5)_2]_2\text{Cl}$, $\text{Fe}[\text{Se}_2\text{CN}(\text{C}_2\text{H}_5)_2]_2\text{Br}$, and $\text{Fe}[\text{Se}_2\text{CN}(\text{C}_2\text{H}_5)_2]_2\text{Cl}$. Extrapolation (solid curves) to $(H/M)_0 = 0$ yields estimates for the critical temperatures.

XY systems having been antiferromagnets (AF's) (Ref. 45). For this reason it is somewhat difficult to make comparisons with earlier systems. Nor are theoretical predictions for the 3D-*XY* model^{46,47} as numerous as those for Ising or Heisenberg models. However, some comparisons with expected *XY* model behavior can be made using the results in Table II and in Fig. 4.

Consider first the ratio of anisotropy fields H_A and H'_A to the exchange field H_E , α and α' in Table II. The out-of-plane anisotropy is very strong, as shown by the large values of α for Fe(dsc)₂Cl and Fe(dsc)₂Br, of the order unity and much larger than values appropriate (≤ 0.01) for a Heisenberg system.³⁵ The in-plane anisotropy, though by no means negligible, is much weaker, as shown by the values of α' , about 20 times smaller than α . This is in marked contrast to the situation for Fe(dtc)₂Cl, where α and α' are both large and of similar magnitude, as can be the case for a system that is Ising-like.³⁵ In fact, a similar ratio of α to α' as that found here for Fe(dsc)₂Cl and Fe(dsc)₂Br, and also with $\alpha \approx 1$, is observed in the well-established 2D-*XY*-AF's CoCl₂·6H₂O and CoBr₂·6H₂O.³⁵

The variation of M/M_0 with T/T_c for Fe(dsc)₂Cl and Fe(dsc)₂Br, shown in Fig. 4, is also informative. It should be noted that although T/T_c is restricted to relatively large values in this diagram this is the most sensitive region for distinguishing one model from another. For both of these bisdsc systems it is apparent that the reduced magnetization increases less sharply as T decreases below T_c than is the case for Fe(dtc)₂Cl. The values derived from the Kouvel-Arrott plot extrapolations are in reasonable agreement with those obtained from Mössbauer data [or from NMR, another microscopic probe, in the case of Fe(dtc)₂Cl], except that the results for Fe(dsc)₂Br are evidently too low. The discrepancy here is possibly due to a relatively large weighing error for the very small (0.89-mg) single crystal employed in the measurements. Apart from this set of results, and allowing for scatter in the other data, it is apparent that for both Fe(dsc)₂Cl and Fe(dsc)₂Br the temperature dependence of the spontaneous magnetization is approximately intermediate between the theoretical curves for the 3D Ising and the 3D H - $S = \frac{1}{2}$ models.^{48,49} We are unaware of any analogous theoretical predictions for the 3D-*XY* model, but based on other results it is reasonable to assume that the temperature dependence of M/M_0 would be intermediate between those of the 3D Ising and Heisenberg models.⁴⁷

The *XY*-type anisotropy which is present in Fe(dsc)₂Cl and Fe(dsc)₂Br can be understood in terms of the anisotropic character of the ground Kramers doublet. The degree of admixture of $|\pm \frac{1}{2}\rangle$ and $|\pm \frac{3}{2}\rangle$ in the actual ground doublet is given by⁵⁰

$$\psi_{1,2} = C_1 |\pm \frac{3}{2}\rangle + C_2 |\mp \frac{1}{2}\rangle, \quad (15)$$

where the coefficients C_1 and C_2 are known functions of D and E (Ref. 50)

$$C_1 = [3E^2/(2D^2 + 6E^2 + \delta D)]^{1/2}, \quad C_2 = (1 - C_1^2)^{1/2}. \quad (16)$$

The resulting values for $C_1 = 0.0174$ and 0.0160 , and $C_2 = 0.9999$ and 0.9999 , for Fe(dsc)₂Cl and Fe(dsc)₂Br,

respectively. Because $D > 0$ and $|E/D|$ is small, the ground doublet turns out to be an almost pure $|\pm \frac{1}{2}\rangle$ state. The upper doublet is a correspondingly pure $|\pm \frac{3}{2}\rangle$ state. The exchange integral is $J/k = 0.37$ K (assuming $\xi = 5$) and is quite small compared to the zero-field splitting δ/k . Thus one anticipates no appreciable additional mixing of the doublets through this interaction. It can further be shown that within the ground doublet, considered as an effective $S' = \frac{1}{2}$ state, the effective g values are⁵⁰

$$\begin{aligned} g'_x &= 2g_x(C_2^2 + 3^{1/2}C_1C_2), \\ g'_y &= 2g_y(C_2^2 - 3^{1/2}C_1C_2), \\ g'_z &= g_z(C_2^2 - 3C_1^2). \end{aligned} \quad (17)$$

The resulting values are $g'_x = 4.40$ and 4.52 , $g'_y = 3.97$ and 4.03 , and $g'_z = 2.09$ and 2.07 , for Fe(dsc)₂Cl and Fe(dsc)₂Br, respectively. It can also be shown that although the true Heisenberg exchange interaction

$$\hat{H}_{ex} = -2J \sum_{(i,j)} \hat{S}_i \cdot \hat{S}_j \quad (18)$$

will normally be isotropic for an orbitally nondegenerate ground state, the effect of the crystal-field anisotropy is to introduce an effective anisotropy into the exchange interaction, which becomes^{46,51}

$$\hat{H}_{ex} = -2 \sum_{(i,j)} J_x \hat{S}'_{ix} \hat{S}'_{jx} + J_y \hat{S}'_{iy} \hat{S}'_{jy} + J_z \hat{S}'_{iz} \hat{S}'_{jz}. \quad (19)$$

The effective exchange constants are related to the true isotropic exchange by⁵¹

$$J_x = (g'_x/g_x)^2 J, \quad J_y = (g'_y/g_y)^2 J, \quad J_z = (g'_z/g_z)^2 J. \quad (20)$$

Apart from the fully isotropic Heisenberg case, two situations are commonly distinguished: (1) $J_z \neq 0$ and $J_x = J_y = 0$, the Ising model, and (2) $J_z = 0$ and $J_x = J_y \neq 0$, the *XY* model. A real system very rarely fulfills these conditions exactly, but is nevertheless often assignable to one of these classes because its overall thermodynamic behavior, and more especially its critical behavior, approximates reasonably well to theoretical predictions for one of the pure models. In a situation where the ground state is 4A_2 , with true spin $\frac{3}{2}$, the Ising model will be approached when $D < 0$ and $E = 0$, so that a pure $|\pm \frac{3}{2}\rangle$ doublet is low-lying. Then when $T \ll \delta/k$, only the lower doublet will be appreciably populated, with effective g values such that $J_x = J_y = 0$ and $J_z = 9J$. This case is approximately fulfilled in Fe(dtc)₂Cl.⁹ The strict *XY* model is more difficult to attain, since even with $D > 0$, $E = 0$, and $T \ll \delta/k$, with $|\pm \frac{1}{2}\rangle$ lowest, there results $J_x = J_y = 4J$ and $J_z = J$. Thus the full *XY* exchange anisotropy is not realized. Nevertheless, even this degree of anisotropy is usually sufficient for *XY* model behavior to be observed.⁴⁵ In the case of Fe(dsc)₂Cl and Fe(dsc)₂Br one estimates that $J_x = 4.24J$, $J_y = 3.76J$, $J_z = J$, and $J_x = 4.22J$, $J_y = 3.78J$, $J_z = J$, respectively. This should be sufficient for *XY* behavior to develop as the upper doublet is depopulated,

though some degree of Ising anisotropy (preferred axis x), apparent in the data and in the nonzero value of α' can also be anticipated.

From the results in Table II it is apparent that the mean exchange interaction in $\text{Fe}(\text{dsc})_2\text{Cl}$ and $\text{Fe}(\text{dsc})_2\text{Br}$ is substantially larger than in the corresponding bisdsc 's by a factor of about 2.3. Although the structures of $\text{Fe}(\text{dsc})_2\text{I}$ and $\text{Fe}(\text{dsc})_2\text{I}$ are, on the available evidence, not isomorphous, the mean exchange interaction is almost twice as large in the selenium system. It should be noted that the value of $\tilde{z}J/k$ for $\text{Fe}(\text{dsc})_2\text{I}$ given in Table II, obtained from the detailed fitting procedure described in Sec. IV, agrees fairly well with that obtained from the molecular-field theory expression³⁵

$$\Theta = 2S(S+1)\tilde{z}J/3k \quad (21)$$

using the observed Weiss constant, $\Theta = -3.52$ K, the result being $\tilde{z}J/k = -1.41$ K. It might also be mentioned that preliminary susceptibility measurements on a polycrystalline sample of $\text{Fe}(\text{dsc})_2\text{Cl}$ were well accounted for between 11 and 80 K by the Curie-Weiss formula, Eq. (10), with $g_{\text{av}} = 2.11$ and $\Theta = 5.04$ K. The g value is consistent with the results in Table II, and the Θ value yields an estimate $\tilde{z}J/k = 2.02$ K, similar to that determined in the detailed fitting of single-crystal data. A reasonable Curie-Weiss fit over an extended temperature range is also an indication that a system is 3D rather than of lower lattice dimensionality.³⁵ The magnitude of the exchange field employed in fitting magnetically perturbed Mössbauer spectra above T_c , 31.5 ± 1.5 and 15 ± 1 kG for $\text{Fe}(\text{dsc})_2\text{Cl}$ and $\text{Fe}(\text{dsc})_2\text{Cl}$, respectively, is also in reasonable agreement, in view of the approximations involved, with the values in Table II obtained from $\tilde{z}J$ using Eq. (14).

Structural considerations do indeed suggest that the exchange interaction should be enhanced in $\text{Fe}(\text{dsc})_2\text{Cl}$ relative to $\text{Fe}(\text{dsc})_2\text{Cl}$. One might normally assume that an increase in covalency would occur by varying a ligand down a group, and that the enhanced delocalization of electron density would yield enhanced superexchange interactions, as is the case for the series MnO , MnS , MnSe .⁵² There may also be some direct evidence for increased covalency in bisdsc 's vs bisdsc 's.¹ The essentially identical Mössbauer quadrupole splittings in $\text{Fe}(\text{dsc})_2\text{Cl}$ and $\text{Fe}(\text{dsc})_2\text{Cl}$, $\Delta E_Q = 2.70$ mm/sec,⁵ provides an indication that the covalency in Fe-S and Fe-Se bonds in these materials is at least similar. We note that purely geometrical considerations suggest an enhancement of near-neighbor intermolecular Se-Se overlap in $\text{Fe}(\text{dsc})_2\text{Cl}$ vs S-S overlap in $\text{Fe}(\text{dsc})_2\text{Cl}$. Such overlaps must be crucial in determining the magnitude of the exchange interaction in these materials, since the separation of the metal ions is too large (≈ 7 Å) for direct exchange to be significant and since no efficient single atom bridge between the metal ions is suggested by the crystal structure of $\text{Fe}(\text{dsc})_2\text{Cl}$. First, the expansion of the unit cell from the dsc to the dsc is 5.2%, so that a typical length element is increased by 1.7%. Consider now the most important intermolecular S-S separations in $\text{Fe}(\text{dsc})_2\text{Cl}$, $r_{\text{SS}} = 3.61, 3.82, 3.84,$ and 4.01 Å.¹⁷ The van der Waals (vdW) radius for sulfur is typically 1.85 Å.⁵³ The ratios $r_{\text{SS}}/2r_{\text{vdW}}(\text{S})$ are 0.976,

1.032, 1.038, and 1.084 in the same order. Ratios less than 1 or at least not much greater than 1 indicate a significant amount of overlap, so that corresponding superexchange interactions involving these S-S contacts are likely to be nontrivial. Now, assuming that positions, sizes, and relative orientations of $\text{Fe}(\text{dsc})_2\text{Cl}$ molecules in their lattice are similar to those of $\text{Fe}(\text{dsc})_2\text{Cl}$ molecules in theirs, one can estimate rather roughly that intermolecular Se-Se separations in $\text{Fe}(\text{dsc})_2\text{Cl}$ will be larger than those in $\text{Fe}(\text{dsc})_2\text{Cl}$ by about 1.017. Yet the vdW radius of Se is typically 2.00 Å, 8% larger than for S.⁵³ Therefore the series of ratios $r_{\text{SeSe}}/2r_{\text{vdW}}(\text{Se})$ is 0.918, 0.971, 0.976, and 1.020, in the same order as before. These ratios are about 6% smaller than those for the dsc . The calculation is obviously very approximate, necessarily so lacking a detailed structure determination for $\text{Fe}(\text{dsc})_2\text{Cl}$. But it seems probable that Se-Se overlap integrals, which will appear squared in theoretical expressions for associated superexchange integrals,⁵² will be larger than corresponding S-S overlaps, and that enhanced exchange interaction in an isomorphous bisdsc relative to the bisdsc is quite likely.

That the dominant exchange interaction in each of $\text{Fe}(\text{dsc})_2\text{Cl}$, $\text{Fe}(\text{dsc})_2\text{Br}$, $\text{Fe}(\text{dsc})_2\text{Cl}$, and $\text{Fe}(\text{dsc})_2\text{Br}$ is ferromagnetic is perhaps slightly surprising. AF exchange is more commonly observed in insulators, and according to the most recent experimental and theoretical work,⁵⁴⁻⁵⁷ more stringent geometrical conditions are associated with ferromagnetic superexchange. However, most of the evidence pertains to single anion bridged systems, where the most important exchange path is of the type $M-X-M$. The characteristics of $M-X \cdots X-M$ bridges have been much less examined. The available evidence suggests that while superexchange interactions across such bridges are also more likely to be AF, the linearity of the bridge will be crucial in determining both the magnitude and the sign of the interaction. Departures from linearity of as little as 30° for dihalide bridges appear to be capable of changing an AF interaction (when linear) to one that is F .⁵⁸ Each of the likely Fe-S(Se) \cdots (Se)S-Fe superexchange paths in the four systems mentioned above is far from being linear. We suspect that this is the qualitative explanation for the dominant ferromagnetism of these materials. In $\text{Fe}(\text{dsc})_2\text{I}$ the most important superexchange paths have not been as clearly identified as in $\text{Fe}(\text{dsc})_2\text{Cl}$, though it is believed that S-S overlaps are the major mechanism for exchange.^{5,17} The structure of the bisdsc and bisdsc iodides are not the same as those of the chlorides and bromides, and it can be assumed that differences in detailed bridge geometry, possibly more linear in the iodides, account for the predominantly AF interactions in these two systems.

It is interesting to consider whether the observed critical temperatures of $\text{Fe}(\text{dsc})_2\text{Cl}$ and $\text{Fe}(\text{dsc})_2\text{Br}$, as well as those of previously examined bisdsc systems, can be accounted for theoretically. The simplest form of mean-field theory is Eq. (21), with $|\Theta|$ identified with T_c . Values calculated from this equation are listed, along with observed T_c 's, in Table III. The usual mean-field theory overestimate of an ordering temperature is clearly evident for the bisdsc 's, but much less evident for the bisdsc 's. One notes that it is only for $\text{Fe}(\text{dsc})_2\text{Cl}$, a negative- D Ising system, that $T_c(\text{obs})$ is clearly larger than the mean-field

TABLE III. Ordering temperatures (in K) of some iron(III)-halide bisdsc and bisdtc systems, and comparison with theoretical values.

System	Observed	Mean field	Series expansion	CEF $\mathcal{J}=5$	CEF $\mathcal{J}=6$
Fe(dsc) ₂ Cl	3.463 (<i>F</i>)	4.62	3.11	3.96	3.15
Fe(dsc) ₂ Br	2.690 (<i>F</i>)	4.62	3.11	3.33	2.74
Fe(dsc) ₂ I	(< 1.3) (<i>AF</i>)	3.88	2.70		
Fe(dtc) ₂ Cl	2.460 (<i>F</i>)	2.02	1.98	2.69	2.30
Fe(dtc) ₂ Br	1.347 (<i>F</i>)	2.00	1.34	1.39	1.14
	1.52				
Fe(dtc) ₂ I	1.937 (<i>AF</i>)	2.00	1.39		

prediction. Certainly a better approach should be to employ series-expansion predictions for the ratio of T_c to J . For cubic Heisenberg ferromagnets and general S , the following semiempirical relation has been obtained,⁵⁹

$$T_c = (\mathcal{J} - 1)(J/k)[0.579S(S+1) - 0.072]. \quad (22)$$

Values obtained from this equation using the $\mathcal{J}J$ in Table II, $S = \frac{3}{2}$, and taking $\mathcal{J}=5$ (rather than the simple cubic $\mathcal{J}=6$, which however, yields T_c 's only 4% higher) are given in Table III in the series-expansion column, for the two ferromagnetic bisdsc's and for Fe(dtc)₂Br. The resulting value for Fe(dtc)₂Cl is 1.36 K. For this Ising system it should presumably be better to use the best available estimate⁶⁰ for a simple cubic, $S = \frac{3}{2}$ Ising ferromagnet, that $kT_c/J' = 2.7127$, where $J' = 2S^2J$ in terms of our J . This is the value, 1.98 K, entered in the table. Had $\mathcal{J}=6$ been assumed, the result would have been $T_c = 1.65$ K. For Heisenberg antiferromagnets an analogous expression to Eq. (22) has been given (Ref. 61) $T_N = T_c[1 + \frac{2}{3}\mathcal{J}S(S+1)]$, where T_c is obtained from Eq. (22). For $S = \frac{3}{2}$ and $\mathcal{J}=5$, this yields a Néel temperature only 3.5% above the corresponding Curie temperature; this is how the values for the two iodide compounds were obtained. Certainly some portions of the discrepancies between observed and calculated ordering temperatures are due to the simple cubic lattice approximation that has been made, but one suspects that additional factors also enter.

In order to obtain yet better agreement the anisotropy must be taken into account in a more satisfactory way. Lines has recently devised a means of estimating the effect of anisotropy on T_c for a wide range of situations, including general S and both negative- D (easy-axis anisotropy) and positive- D (easy-plane anisotropy), within the context of a correlated effective field (CEF) theory.⁶² The results of this approach appear to be inferior only to exact high-temperature series-expansion predictions (not available for the cases of interest here) and to diagrammatic Green's-function calculations⁶³ (not yet applied for $S = \frac{3}{2}$ and general anisotropy). In the last two columns of Table III we enter the values of T_c obtained for the four ferromagnets (the antiferromagnetic case can be but has not yet been treated) as estimated from Lines's plots of kT_c/JS^2 vs D/J for a simple cubic lattice. Again, a lattice approxi-

mation must be made, and in order to obtain a feeling for the sort of error that might accompany this, we have entered the results by assuming either $\mathcal{J}=5$ or $\mathcal{J}=6$. It appears that taking $\mathcal{J}=6$ leads to better overall agreement with the observed ordering temperatures. That the $\mathcal{J}=6$ prediction is below that observed for Fe(dtc)₂Cl is possibly encouraging, since an underestimate appears to be expected in applying the theory to a large negative D/J situation. Except in the case of Fe(dtc)₂Br, the $\mathcal{J}=6$ CEF predictions are an improvement over the series-expansion predictions. It should be noted that neither the CEF nor any other theory incorporates an $E(\hat{S}_x^2 - \hat{S}_y^2)$ anisotropy term, which might be significant for the bisdtc's especially. In view of the approximations involved, the agreement is probably quite satisfactory.

A few remarks concerning the zero-field splitting parameters determined in this and earlier work are appropriate. D for Fe(dsc)₂Br is found to be substantially larger than for Fe(dsc)₂Cl. A larger zero-field splitting in an isostructural bromide complex, relative to the chloride homolog, is almost invariably observed.⁶⁴ This can be rationalized on theoretical grounds, the primary factor being the relative covalency of the $M-X$ bond.⁶⁵ For the same reason then, it is expected that the D value and zero-field splitting for an isostructural iodide should be larger yet. This trend is observed in a recently examined high-spin iron(III) porphyrin series.⁶⁴ The prediction appears to be fulfilled in the entire bisdtc series under consideration here, but may fail for the bisdsc iodide. However, it is also known that small structural variations can have a pronounced effect on the magnitude and sign of the zero-field splitting parameter D .⁶⁶ Since the crystal structure and precise molecular geometry of Fe(dsc)₂I are at present unknown, and since moreover the zero-field splitting parameters listed for this system in Table II are less reliably determined, a final judgment on the regularity of the variation of D with halide in the bisdsc series should obviously be postponed. Along similar lines it may also be observed that, with the possible exception of Fe(dsc)₂I, the zero-field splitting is substantially larger in a bisdsc halide complex than in the corresponding bisdtc. Again, the probably somewhat greater covalency of Fe-Se relative to Fe-S bonds is very likely a major determining factor here.

In conclusion, we consider the apparent saturation moments of Fe(dsc)₂Cl and Fe(dsc)₂Br: $2.85\mu_B/\text{ion}$ and $2.75\mu_B/\text{ion}$, respectively. These values may be compared

with the moments computed for a system exposed to the exchange fields listed in Table II. Using the appropriate crystal-field parameters and magnetic fields applied parallel to the x axis of Eq. (4), we find the values $2.80\mu_B/\text{ion}$ and $2.45\mu_B/\text{ion}$ for $\text{Fe}(\text{dsc})_2\text{Cl}$ and $\text{Fe}(\text{dsc})_2\text{Br}$. The value for $\text{Fe}(\text{dsc})_2\text{Cl}$ is in excellent agreement with experiment. The value for $\text{Fe}(\text{dsc})_2\text{Br}$ is only slightly below experiment. In either case, they are significantly smaller than the observed moment in $\text{Fe}(\text{dtc})_2\text{Cl}$, $3.12\mu_B/\text{ion}$. Thus in dtc or dsc complexes with $T_c < 4$ K, the saturation moments alone are a useful indicator of Ising versus XY character.

ACKNOWLEDGMENTS

The work at Oregon State University has been supported by National Science Foundation Grant No. DMR-78-08452. The work at the College of William and Mary has been supported by a grant from the Thomas F. Jeffress and Kate Miller Jeffress Memorial Trust. Grateful acknowledgment is also made to the donors of the Petroleum Research Fund, administered by the American Chemical Society, for support of this research, and to the Research Corporation and the National Science Foundation, Grant No. PRM-81-07444, for equipment grants (G.C.D.).

- ¹E. Cervone, F. Diomedei Camassei, M. L. Luciani, and C. Furlani, *J. Inorg. Nucl. Chem.* **31**, 1101 (1969).
- ²F. V. Wells, Ph.D. thesis, Oregon State University, 1984.
- ³R. L. Martin and A. H. White, *Inorg. Chem.* **6**, 712 (1967).
- ⁴H. H. Wickman and A. M. Trozzolo, *Inorg. Chem.* **7**, 63 (1968).
- ⁵G. E. Chapps, S. W. McCann, H. H. Wickman, and R. C. Sherwood, *J. Chem. Phys.* **60**, 990 (1974).
- ⁶P. Ganguli, V. R. Marathe, and S. Mitra, *Inorg. Chem.* **14**, 970 (1975).
- ⁷D. Petridis, A. Simopoulos, A. Kostikas, and M. Pasternak, *J. Chem. Phys.* **65**, 3139 (1976).
- ⁸A. Malliaris and V. Petrouleas, *J. Phys. (Paris) Colloq.* **37**, C6-101 (1976).
- ⁹G. C. DeFotis, F. Palacio, and R. L. Carlin, *Phys. Rev. B* **20**, 2945 (1979).
- ¹⁰G. C. DeFotis and J. A. Cowen, *J. Chem. Phys.* **73**, 2120 (1980).
- ¹¹S. Decurtins, F. V. Wells, K. C.-P. Sun, and H. H. Wickman, *Chem. Phys. Lett.* **89**, 79 (1982).
- ¹²M. Yoshikawa, M. Sorai, H. Suga, and S. Seki, *J. Phys. Chem. Solids* **41**, 1295 (1980).
- ¹³M. Yoshikawa, M. Sorai, H. Suga, and S. Seki, *J. Phys. Chem. Solids* **44**, 311 (1983).
- ¹⁴H. H. Wickman, A. M. Trozzolo, H. J. Williams, G. W. Hull, and F. R. Merritt, *Phys. Rev.* **155**, 563 (1967).
- ¹⁵N. Arai, M. Sorai, H. Suga, and S. Seki, *J. Phys. Chem. Solids* **38**, 1341 (1977).
- ¹⁶H. H. Wickman and C. F. Wagner, *J. Chem. Phys.* **51**, 435 (1969).
- ¹⁷H. H. Wickman, *J. Chem. Phys.* **56**, 976 (1972).
- ¹⁸G. C. DeFotis, F. Palacio, and R. L. Carlin, *Physica* **95B**, 380 (1978).
- ¹⁹G. C. DeFotis and S. A. Pugh, *Phys. Rev. B* **24**, 6497 (1981).
- ²⁰A. Malliaris, A. Kostikas, and A. Simopoulos, *Chem. Phys. Lett.* **28**, 608 (1974).
- ²¹A. Malliaris and D. Petridis, *Chem. Phys. Lett.* **36**, 117 (1975).
- ²²A. Malliaris and A. Simopoulos, *J. Chem. Phys.* **63**, 595 (1975).
- ²³S. Decurtins (private communication).
- ²⁴B. F. Hoskins and A. H. White, *J. Chem. Soc. A*, 1668 (1970).
- ²⁵P. C. Healy, A. H. White, and B. F. Hoskins, *J. Chem. Soc. D*, 1369 (1972).
- ²⁶G. C. DeFotis, *Rev. Sci. Instrum.* **54**, 248 (1983).
- ²⁷J. M. Grow, G. L. Robbins, and H. H. Wickman, *J. Phys. (Paris) Colloq.* **37**, C6-633 (1976).
- ²⁸V. R. Marathe, A. Trautwein, and A. Kostikas, *J. Phys. (Paris) Colloq.* **41**, C1-315 (1980).
- ²⁹P. Ganguli and K. M. Hasselback, *Z. Naturforsch.* **34A**, 1500 (1979).
- ³⁰F. V. Wells and H. H. Wickman (unpublished).
- ³¹J. N. McElearney, G. E. Shankle, R. W. Schwartz, and R. L. Carlin, *J. Chem. Phys.* **56**, 3755 (1972).
- ³²J. W. Stout and W. B. Hadley, *J. Chem. Phys.* **40**, 55 (1964).
- ³³H. H. Wickman, M. P. Klein, and D. A. Shirley, *J. Chem. Phys.* **42**, 2113 (1965).
- ³⁴E. Velu, J.-P. Renard, and B. Lecuyer, *Phys. Rev. B* **14**, 5088 (1976).
- ³⁵L. J. de Jongh and A. R. Miedema, *Experiments on Simple Magnetic Model Systems* (Taylor and Francis, London, 1974), pp. 20, 63, 145, 86, 71, 37, and 133.
- ³⁶W. E. Estes, D. B. Losee, and W. E. Hatfield, *J. Chem. Phys.* **72**, 630 (1980).
- ³⁷A. H. Morrish, *The Physical Principles of Magnetism* (Wiley, New York, 1965), p. 320.
- ³⁸A. Arrott, *Phys. Rev.* **108**, 1394 (1957).
- ³⁹R. C. Chisholm and J. W. Stout, *J. Chem. Phys.* **36**, 972 (1962).
- ⁴⁰I. S. Jacobs, S. Roberts, and S. D. Silverstein, *J. Appl. Phys.* **39**, 816 (1968).
- ⁴¹A. Dupas, K. LeDang, J.-P. Renard, P. Veillet, A. Daoud, and R. Perret, *J. Chem. Phys.* **65**, 4099 (1976).
- ⁴²R. D. Willett, F. H. Jardine, I. Rouse, R. J. Wong, C. P. Landee, and M. Numata, *Phys. Rev. B* **24**, 5372 (1981).
- ⁴³G. E. Davidson, M. Eibschütz, D. E. Cox, and J. Minkiewicz, in *Magnetism and Magnetic Materials—1971 (Chicago)*, Proceedings of the 17th Annual Conference on Magnetism and Magnetic Materials, edited by C. D. Graham and J. J. Rhyne (AIP, New York, 1971), p. 436.
- ⁴⁴M. Steiner, W. Kruger, and D. Babel, *Solid State Commun.* **9**, 227 (1971).
- ⁴⁵A. van der Bilt, K. O. Joung, R. L. Carlin, and L. J. de Jongh, *Phys. Rev. B* **24**, 445 (1981), and references to related systems therein.
- ⁴⁶D. D. Betts, in *Phase Transitions and Critical Phenomena*, edited by C. Domb and M. S. Green (Academic, New York, 1974), Vol. 3, p. 569.
- ⁴⁷D. D. Betts, *Physica* **86B-88B**, 556 (1977).
- ⁴⁸P. F. Fox and A. J. Guttman, *J. Phys. C* **6**, 913 (1973).
- ⁴⁹G. A. Baker, Jr., J. Eve, and G. S. Rushbrooke, *Phys. Rev. B* **2**, 706 (1970).
- ⁵⁰G. E. Shankle, J. N. McElearney, R. W. Schwartz, A. R. Kampf, and R. L. Carlin, *J. Chem. Phys.* **56**, 3750 (1972).

- ⁵¹M. E. Lines, *Phys. Rev.* **131**, 546 (1963).
- ⁵²N. Menyuk, in *Modern Aspects of Solid State Chemistry*, edited by C. N. R. Rao (Plenum, New York, 1970), p. 200.
- ⁵³L. Pauling, *The Nature of the Chemical Bond*, 3rd ed. (Cornell University Press, Ithaca, 1960), p. 260.
- ⁵⁴V. H. Crawford, H. W. Richardson, J. R. Wasson, D. J. Hodgson, and W. E. Hatfield, *Inorg. Chem.* **15**, 2107 (1976).
- ⁵⁵R. D. Willett and C. P. Landee, *J. Appl. Phys.* **52**, 2004 (1981).
- ⁵⁶P. J. Hay, J. C. Thibeault, and R. Hoffmann, *J. Am. Chem. Soc.* **97**, 4884 (1975).
- ⁵⁷O. Kahn, J. Galy, Y. Journaux, J. Jaud, and I. Morgenstern-Badarau, *J. Am. Chem. Soc.* **104**, 2165 (1982).
- ⁵⁸R. Block and L. Jansen, *Phys. Rev. B* **26**, 148 (1982).
- ⁵⁹G. S. Rushbrooke, G. A. Baker, Jr., and P. J. Wood, in *Phase Transitions and Critical Phenomena*, edited by C. Domb and M. S. Green (Academic, New York, 1974), Vol. 3, p. 306.
- ⁶⁰W. J. Camp and J. P. Van Dyke, *Phys. Rev. B* **11**, 2579 (1975).
- ⁶¹G. S. Rushbrooke and P. J. Wood, *Mol. Phys.* **6**, 409 (1963).
- ⁶²M. E. Lines, *Phys. Rev. B* **12**, 3766 (1975).
- ⁶³D. H.-Y. Yang and Y.-L. Wang, *Phys. Rev. B* **12**, 1057 (1975).
- ⁶⁴D. V. Behere, S. K. Date, and S. Mitra, *Chem. Phys. Lett.* **68**, 544 (1979).
- ⁶⁵M. Heming and G. Lehmann, *Chem. Phys. Lett.* **80**, 235 (1981).
- ⁶⁶W. DeW. Horrocks, Jr. and D. A. Burlone, *J. Am. Chem. Soc.* **98**, 6512 (1976).